Chinese Physics B

PAPER

Achieving ultracold Bose–Fermi mixture of ^{87}Rb and ^{40}K with dual dark magnetic-optical-trap

To cite this article: Jie Miao *et al* 2022 *Chinese Phys. B* **31** 080306

Achieving ultracold Bose–Fermi mixture of ^{87}Rb and ^{40}K with dual dark magnetic-optical-trap

Jie Miao(苗杰)[1,2], Guoqi Bian(边国旗)[1,2], Biao Shan(单标)[1,2], Liangchao Chen(陈良超)[1,2], Zengming Meng(孟增明)[1,2], Pengjun Wang(王鹏军)[1,2], Lianghui Huang(黄良辉)[1,2,†], and Jing Zhang(张靖)[1,2,‡]

[1] *State Key Laboratory of Quantum Optics and Quantum Optics Devices, Institute of Opto-electronics, Shanxi University, Taiyuan* 030006, *China*
[2] *Collaborative Innovation Center of Extreme Optics, Shanxi University, Taiyuan* 030006, *China*

(Received 21 January 2022; revised manuscript received 21 February 2022; accepted manuscript online 25 February 2022)

We demonstrate that dual dark magnetic-optical-traps (MOTs) have great importance in the two-species ^{87}Rb and ^{40}K mixture compared with dual bright MOTs. The dark MOT has a little improvement in the trapping of single-species ^{87}Rb or ^{40}K gases compared with bright MOT. For the case of loading two-species ^{87}Rb and ^{40}K simultaneously, the improvement of ^{40}K in the dual dark MOTs is mainly from the reduction of light-assisted collision losses. The dual dark MOTs employ a pair of conical lenses to produce the hollow beam for repump laser with high efficiency. The number and density of ^{87}Rb and ^{40}K atoms after evaporative cooling in the hybrid magnetic trap with dark MOT loading are compared with those in bright MOT. The atoms with large number and high density make it easier to realize the quantum degenerate of Bose–Fermi mixture.

Keywords: Bose–Fermi mixture, dark magnetic-optical-trap (MOT), Fermi gas, hollow beam

PACS: 03.75.Ss, 37.10.De, 34.50.Cx, 67.85.Pq **DOI:** 10.1088/1674-1056/ac5882

Since the invention of laser cooling, high-density ultracold atomic vapors can be achieved easily and applied in many fields such as quantum precision measurement, cold atomic clock,[1] atom interferometry,[2,3] and quantum optics.[4] The emergence of evaporative cooling to overcome the laser cooling limitations makes the ultracold atomic vapors reach quantum degeneracy.[5] Quantum degenerate gases provide a unique platform for broad field.[6,7] The atomic vapors can be cooled to the quantum degenerate state usually by a standard procedure of magnetic-optical-trap (MOT),[8] optical molasses, optical pump and evaporative cooling.[9–12] Larger number and higher density of atoms with high loading rate in magnetic trap or optical trap are good starting point for the application of quantum degenerate gases. Therefore, many new cooling technologies were developed, such as dark MOT, narrow-line laser cooling,[13] gray molasses,[14] Raman cooling,[15] 3D Raman sideband cooling,[16] and direct laser cooling[17,18] to quantum degenerate.

The bright MOT has the limit that the numbers and density are reduced due to light-assisted collision losses.[19,20] In order to reduce this loss, the dark spontaneous-force optical trap (or called dark MOT) has been demonstrated by Wolfgang Ketterle and his colleagues in 1993 for the first time and used in sodium, in which the number of atoms can reached 10^{10} and the density of atoms reached to 10^{12} cm^{-3}.[21] Dark MOT confines most of the atoms in the hyperfine ground state which does not interact with the cooling light. Therefore, this hyperfine ground state is the so-called dark state.[21] Dark MOT is produced by strongly reducing or blocking the laser intensity in the central part of the repumping laser beam, which makes the atoms gather in the dark hyperfine ground state (without the interaction with the cooling light) and spend most of their time. The atoms in the dark hyperfine ground state are accumulated in the center of MOT due to trapping force, so the density of the atoms gets improved. Thus, dark MOT becomes an important cooling method to be applied especially in realizing the atomic mixture, which can load two atomic species simultaneously to avoid the light-assisted collision losses between two atomic species.[21]

In this paper, we demonstrate the realizing of ultracold Bose–Fermi mixture of ^{87}Rb and ^{40}K employing the technology of dual dark MOTs. Compared with bright MOT, ^{40}K numbers and density get significantly improved in loading two species of ^{87}Rb and ^{40}K simultaneously via dark MOT. However, dark MOT has no improvement only for loading of the single species of ^{87}Rb and the numbers and density of single species ^{40}K are slightly improved. Two species of ^{87}Rb and ^{40}K are loaded by means of two different times in the period of dark MOT. The mixing ratio of ^{87}Rb and ^{40}K in two-species mixture can be adjusted easily by controlling the different MOT loading times of ^{87}Rb and ^{40}K.

The experimental set up is shown in Fig. 1, composed of dual MOTs (2D MOT + 3D MOT configurations) for ^{87}Rb and ^{40}K. The 2D MOT chamber is composed of four rectangular light windows with a size of 150 mm×50 mm. Each of the four windows has rectangular coils on the outside to generate a

†Corresponding author. E-mail: huanglh06@126.com
‡Corresponding author. E-mail: jzhang74@yahoo.com; jzhang74@sxu.edu.cn

two-dimensional quadrupole magnetic field. The front part of 2D chamber has a circular window for push light, and the back part is connected to the 3D science cell via a flange, in which a differential tube is installed. The differential tube is used to maintain a vapor pressure between 2D chamber and 3D science cell. The 2D light entering from the 2D window and returning multiple times is combined with the two-dimensional quadrupole magnetic field to form a 2D MOT.

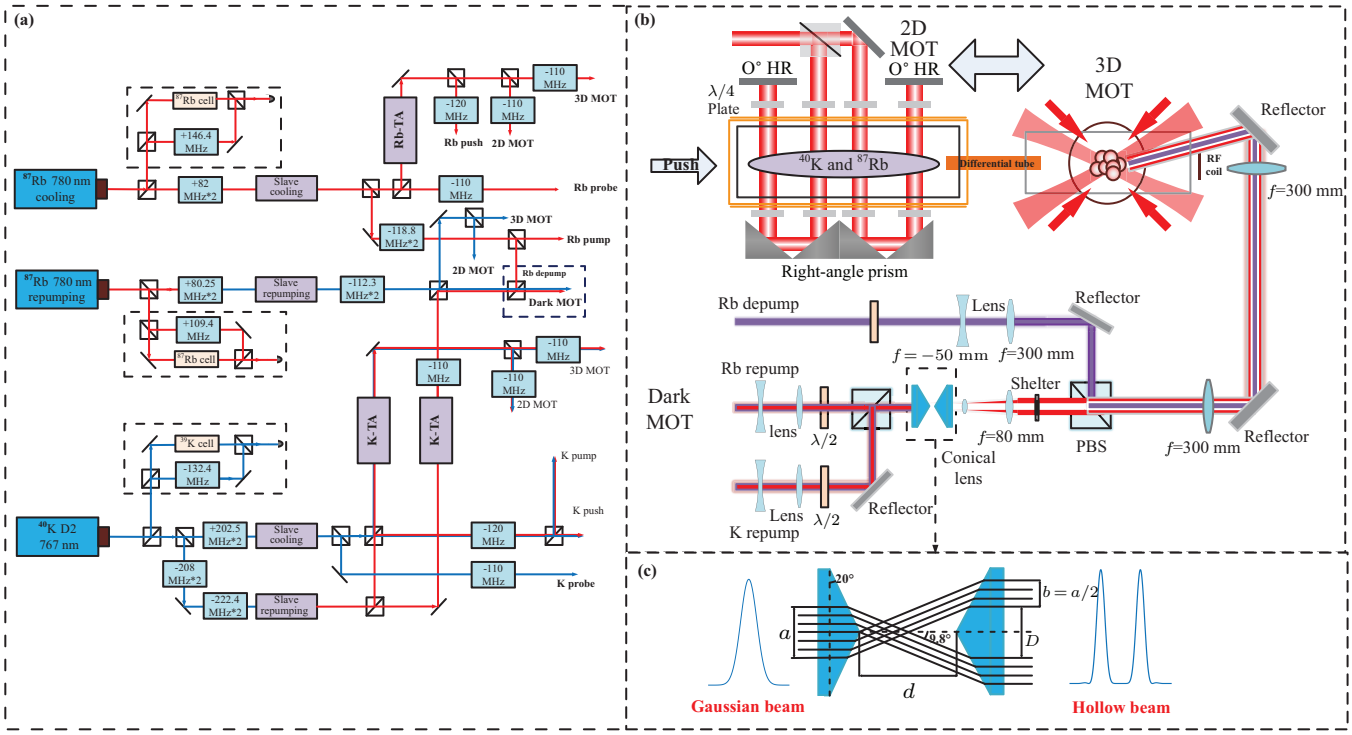

Fig. 1. (a) The optical setup, frequency shifting, locking schemes of the ^{87}Rb and ^{40}K cooling light and repumping light. (b) The schematic of 2D MOT, 3D MOT and the optical setup of dual dark MOT of ^{87}Rb and ^{40}K. The differential tube is used to maintain the pressure of 2D cell chamber and 3D science cell. A push laser is used for transferring atoms from 2D MOT to 3D MOT. The RF coil is used for evaporation of atoms. The crossed optical dipole trap is generated by two 1064 nm laser light. (c) The generation of hollow beam for repumping light. The Gaussian beam is converted into the hollow beam via a pairs of conical lens.

The 3D MOT science cell is a glass cell with a size of 40 mm × 40 mm × 100 mm. The 3D MOT region is located by a pair of coils in the anti-Helmholtz configuration which provide the 3D magnetic quadrupole field. The six individual laser beams from six directions are combined with the 3D magnetic quadrupole field to generate the 3D MOT. The vapor pressure of the 2D chamber and the 3D science cell are maintained at $\sim 10^{-7}$ Pa and $\sim 10^{-9}$ Pa, respectively.

Experimentally, we need different laser frequencies for ^{87}Rb and ^{40}K during different stages. An overview of the laser frequencies required for both isotopes is given in Table 1. The center wavelengths of the three master lasers (including two lasers are for cooling and repumping light of ^{87}Rb respectively and one is ^{40}K) are 780 nm and 767 nm corresponding to the D2 lines as shown in Fig. 2.[22] The master laser for ^{40}K is divided into two parts, which are frequency-shifted as the cooling light and repumping light by acousto-optic modulators (AOMs). The modulation transfer spectroscopy is used to stabilize the frequency of the three master lasers (K master laser is locked at ^{39}K absorption line). The advantage of this configuration is to avoid the modulation on the master laser.[23,24] Then all lights produced by three master lasers are transmitted via polarization-maintaining optical fiber and injected into the four slave lasers with the configuration of injection locked laser diode. At last, three tapered amplifiers (cooling and repumping light of ^{40}K and cooling light of ^{87}Rb) are seeded by slave laser for the second amplification to match the laser power requirement of our experiment.[25] The generation and combination of different laser frequencies for cooling, repumping, pump, push and detection of two atomic species via beam splitter and different AOM frequency shift are described in Fig. 1(a).

The important novelty in our dark MOT is that we use one pair of conical lens to produce a hollow beam for repumping light[26–28] as shown in Fig. 1(b). Usually, a hollow repumping light is generated by passing through a glass plate with a black dot in the center directly. Compared with this simple way, most power of repumping light at central area in our work is transferred to the outside ring area instead of lost. Moreover, we can control the blocking area easily by adjusting the distance between two conical lenses in Fig. 1(c). Both repumping light ^{87}Rb and ^{40}K are coupled together by PBS and then pass through a pair of conical lens to transform a collimated gaussian beam into a hollow beam.[29] The hollow

beam is expanded by the telescope system to an outer diameter of ~ 30 mm, and the inner diameter of ~ 10 mm. Then we use a mask to further suppress the beam intensity at the center of ring. We have used a $4f$ system to image the dark spot into the center of 3D MOT. For ^{87}Rb, a depumping light from transition $|5S_{1/2}, F = 2\rangle$ to $|5P_{3/2}, F = 2\rangle$ is added to deplete atoms in $|F = 2\rangle$ state in the center of the MOT via optical pumping the atoms go back to $|5S_{1/2}, F = 1\rangle$ state. The diameter of the depumping beam is expanded to 10 mm by using the combination of lens with focal lengths of -50 mm and 300 mm, which fit the dark region of the hollow beam of the dark MOT, so that the light has better interaction with the atoms. After optimization, repumping and depumping power are 15 mW and 4.6 mW for the dark MOT of ^{87}Rb respectively, and the repumping power is 85 mW for the dark MOT of ^{40}K.

Table 1. Laser frequencies used in cooling and trapping of ^{87}Rb and ^{40}K ($\Gamma \sim 6$ MHz).

	^{87}Rb	
Light	Frequency	Detuning
Cooling light	$5^2S_{1/2}F = 2 \rightarrow 5^2P_{3/2}F = 3$	-2.2Γ
Repumping light	$5^2S_{1/2}F = 1 \rightarrow 5^2P_{3/2}F = 2$	-5.13Γ
Probe light	$5^2S_{1/2}F = 2 \rightarrow 5^2P_{3/2}F = 3$	resonant
Pump light	$5^2S_{1/2}F = 2 \rightarrow 5^2P_{3/2}F = 2$	$+1.6\Gamma$
Push light	$5^2S_{1/2}F = 2 \rightarrow 5^2P_{3/2}F = 3$	-4.93Γ
	^{40}K	
Light	Frequency	Detuning
Cooling light	$4^2S_{1/2}F = 9/2 \rightarrow 4^2P_{3/2}F = 11/2$	-2.6Γ
Repumping light	$4^2S_{1/2}F = 7/2 \rightarrow 4^2P_{3/2}F = 9/2$	-2.2Γ
Probe light	$4^2S_{1/2}F = 9/2 \rightarrow 4^2P_{3/2}F = 11/2$	resonant
Pump light	$4^2S_{1/2}F = 9/2 \rightarrow 4^2P_{3/2}F = 9/2$	-3.78Γ
Push light	$4^2S_{1/2}F = 9/2 \rightarrow 4^2P_{3/2}F = 11/2$	-1.76Γ

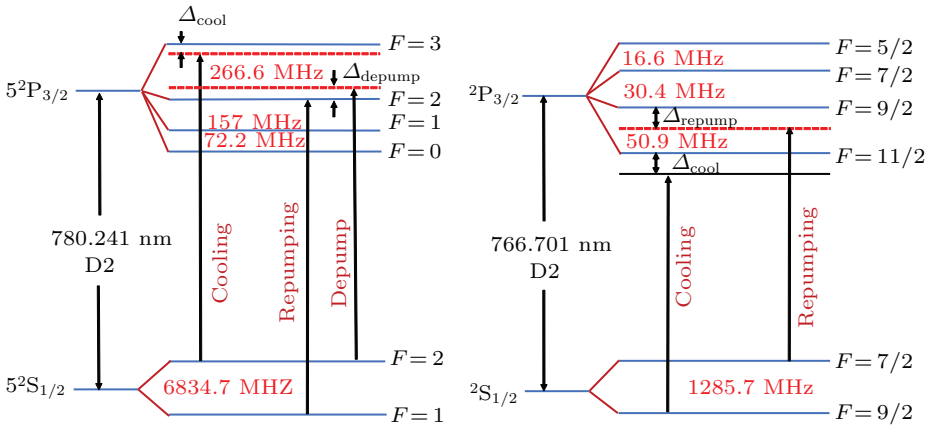

Fig. 2. Hyperfine structure of D2-line of ^{87}Rb and ^{40}K. (a) Transitions of ^{87}Rb D2 line for the cooling light, repump light and depump light. (b) Transitions of ^{40}K D2 line for the cooling and repump light.

Two species of ^{87}Rb and ^{40}K are loaded by means of two different time sequences in the period of dark MOT and the time sequences are shown in Fig. 3. The mixing ratio of ^{87} Rb and ^{40}K in the two-species mixture can be adjusted easily by controlling the different MOT loading times of ^{87} Rb and ^{40}K. Firstly, the ^{40}K atoms are only loaded in 3D dark MOT that lasts for 60 s. During this stage, a transversal and slow atomic beam is generated in the 2D MOT and then transferred to the 3D MOT via a push beam. We use the $F = 9/2 \longrightarrow F' = 11/2$ cycling transition for trapping and cooling of ^{40}K and the $F = 7/2 \longrightarrow F' = 9/2$ for repumping. The atoms gather in the "dark" state $F = 7/2$. Sequently, we keep laser light of ^{40}K unchanged and open the 2D laser light and 3D dark MOT laser light of ^{87}Rb, then the ^{87}Rb atoms can be simultaneously loaded in 3D MOT within 5 s. For ^{87}Rb atom's 3D dark MOT loading, we use the $F = 2 \longrightarrow F' = 3$ cycling transition for trapping and cooling, and the $F = 1 \longrightarrow F' = 2$ for repumping. At last, the atoms gather in the center region with the "dark" state $F = 1$ to avoid the light-assisted losses with the "dark" state $F = 7/2$ of ^{40}K atoms. Thus, the larger number of atoms and higher density for Rb–K mixture can be obtained by dual dark MOT, which is the main result in this paper.

Then, the standard procedures of polarization gradient cooling (optical molasses), optical pumping are performed. Before optical molasses, the push laser and the magnetic field of 2D MOT are switched off. Then depump beam of ^{87}Rb is switched off, and the intensity of ^{87}Rb cooling light and ^{40}K cooling light is reduced to 90% of the original intensity. Meanwhile, the configuration of the repumping light switches from the single hollow beam to the six directions by using the standard bright MOT. The detuning of cooling and repumping lasers of ^{40}K and ^{87}Rb for 3D MOT are given in Fig. 3. This process lasts for 10 ms with the quadrupole magnetic field keeping constant at 9 G/cm (which is the same as the dark 3D MOT loading). Till now, we complete the conversion from dark MOT to bright MOT. During optical molasses, the magnetic field is quickly switched off and the stray magnetic field is compensated to be 0 by three pairs of larger Helmholtz coils. When the laser detunings are set as shown in Fig. 3, we perform a 3 ms polarization gradient cooling phase with the counterpropagating σ^+ and σ^- circularly polarised MOT beams.[30] Right after the molasses step, we use a magnetic

guiding field of 1 G for optical pumping. And ^{40}K and ^{87}Rb atoms are optically pumped into the weak-field seeking Zeeman state $|F=2,m_{\rm f}=2\rangle$ and $|F=9/2,m_{\rm f}=9/2\rangle$ within 500 μs, which make ^{40}K and ^{87}Rb atoms be easily trapped in the hybrid magnetic trap. The 18 W green laser is turned on at full power focused at the center of the magnetic quadrupole trap to generate the optically plugged magnetic quadrupole trap (hybrid magnetic trap) in order to avoid Majorana losses. After trapping the atoms in hybrid magnetic trap, the density of atoms is increased and the temperature of atoms is further decreased with the elastic collisions in the following radio-frequency (RF) evaporation stage.

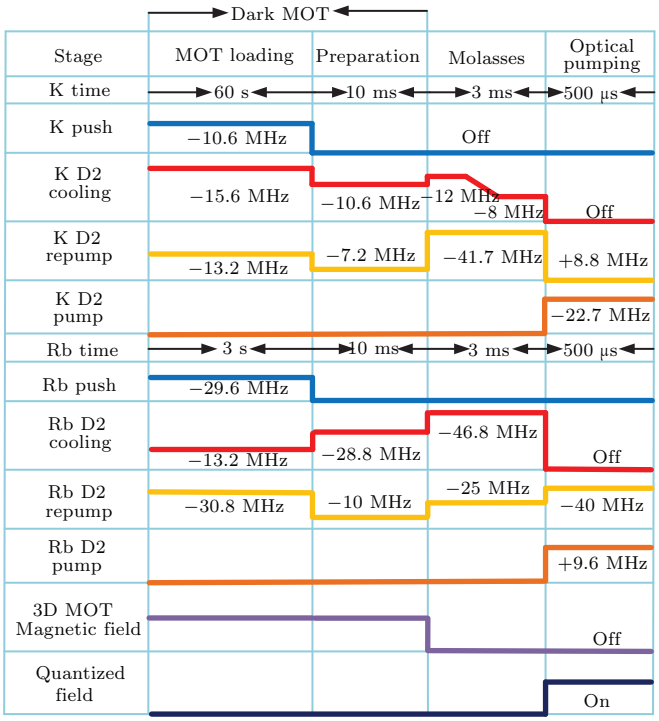

Fig. 3. Time sequences of the cooling process at different stages.

In the stage of RF evaporation, the ^{87}Rb atoms has been adiabatically transformed from the weak-field seeking state $|F=2,m_{\rm f}=2\rangle$ to the high-field seeking state $|F=2,m_{\rm f}=-2\rangle$ by a sequence of induced spin flips and the radio frequency is swept from 27 MHz to 1.5 MHz with a few linear ramps in 12 s. In order to cool sympathetically the fermionic ^{40}K atoms in the $|F=9/2,m_{\rm f}=9/2\rangle$ state by a bath of bosonic ^{87}Rb in the $|F=2,m_{\rm f}=2\rangle$ state, the key mechanism is the collision between Bose gas ^{87}Rb and Fermi gas ^{40}K.[31] There is the large and negative scattering length with $(-215\pm10)\,a_0$ between ^{40}K and ^{87}Rb in the above mentioned spin states, which ensures an efficient rethermalization.[32] Here, the mixture ratio of ^{87}Rb numbers and ^{40}K numbers is the crucial factor to keep the high evaporation efficiency of ^{40}K in the sympathetical cooling, thus the number of ^{87}Rb atoms and ^{40}K atoms are accurately adjusted by the loading time of ^{87}Rb and ^{40}K.

The atomic gases are typically imaged on charge couple device (CCD) camera by the time-of-flight (TOF) absorption to gain atomic information including atom numbers and optical density. For absorption imaging, we use the closed transition $|F=2\rangle\rightarrow|F'=3\rangle$ and $|F=9/2\rangle\rightarrow|F'=11/2\rangle$ for detection of ^{87}Rb and ^{40}K, respectively. The ^{87}Rb cloud is typically imaged after 15 ms time of flight, whereas 2 ms time of flight for the ^{40}K cloud. The relationship between the optical density and the density of atoms is as follows:

$$D(x,y)=\sigma\int n(x,y,z)\,{\rm d}z, \tag{1}$$

where σ is the atomic scattering cross section and $n(x,y,z)$ is number of atoms density distribution. We can know that high optical density represents the high atomic density from Eq. (1).

Here we compare dark MOT loading with bright MOT by measuring the number of atoms and densities of ^{87}Rb and ^{40}K after evaporation in hybrid magnetic trap. Firstly, we only consider ^{87}Rb atoms loading and evaporation cooling. The number and density of ^{87}Rb atoms as the function of the different loading times are shown in Fig. 4. The red dot and black dot represent dark MOT loading and bright MOT loading, respectively. The atomic gas of single-species of ^{87}Rb after evaporation in hybrid magnetic trap can reach the saturation after about 10 s both for dark and bright MOT loading. The number of atoms can reach the 6.5×10^7 and the optical density can reach 2.6. So that our result shows that the dark MOT loading is the same as bright MOT loading for single specie ^{87}Rb gas.

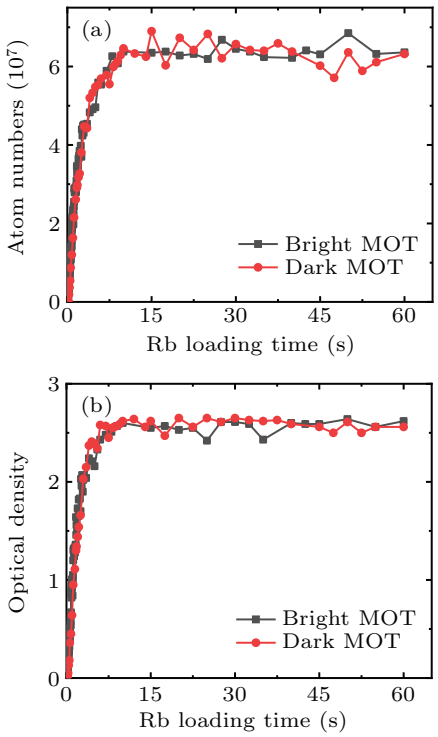

Fig. 4. ^{87}Rb number (a) and density (b) after evaporation as the function of loading time via two different MOT loading. The number of atoms and density after evaporation in hybrid magnetic trap with dark MOT loading and bright MOT loading are basically same for single species of ^{87}Rb atoms.

Next, we consider loading of ^{40}K atoms and ^{87}Rb atoms simultaneously. In this progress, we keep the loading time of ^{87}Rb constant at 5 s. The number of atoms and optical density of ^{40}K as the function of the different loading time is shown in Figs. 5(a) and 5(b), respectively. The red dot and black dot represent dark MOT loading and bright MOT loading, respectively. The atomic gas of ^{40}K in two-species ^{87}Rb and ^{40}K mixture after evaporation reach the saturation after about 40 s for bright MOT loading and about 120 s for dark MOT loading. The number of ^{40}K atoms with dark MOT loading is more than three times as much as bright MOT loading, and the optical density is more than two times. Based on our results, dark MOT loading shows great improvements for the ^{40}K number of atoms and density in two-species ^{87}Rb and ^{40}K.

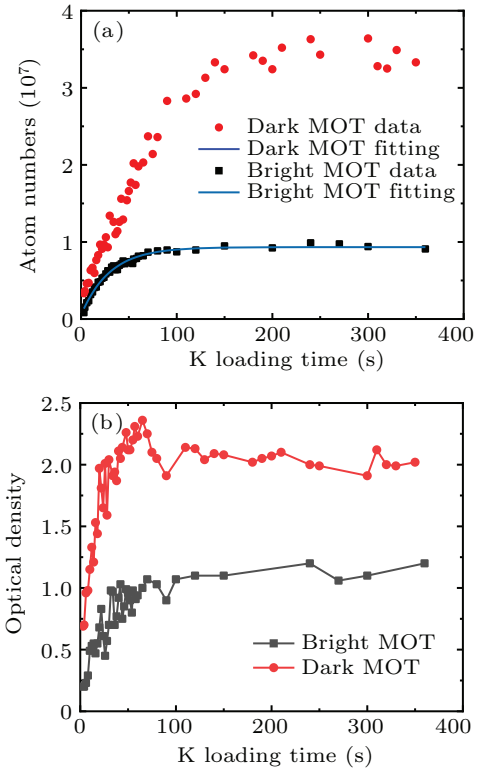

Fig. 5. The ^{40}K atom numbers and density after evaporation as the function of loading time via two different MOT loading. Here, the loading time of ^{87}Rb is constant with 5 s. The red and black dots represent the data of loading atoms via dark MOT loading and bright MOT loading, the solid lines are the fits using Eq. (2).

The loading process for the K MOT in the presence of the Rb atoms is given by the following rate equation:

$$\frac{\mathrm{d}N_{\mathrm{K}}}{\mathrm{d}t} = L - \gamma N_{\mathrm{K}} - \beta \int n_{\mathrm{K}}^2 \,\mathrm{d}^3 r - \beta' \int n_{\mathrm{K}} n_{\mathrm{Rb}} \,\mathrm{d}^3 r, \qquad (2)$$

where L is the loading rate, γ is the loss rate caused by collisions between the trapped K atoms and the hot background, β is the loss rate resulting from collisions among the trapped potassium atoms, β' is the loss rate due to collisions between trapped potassium and rubidium, n_{K} and n_{Rb} are the density of potassium and rubidium atoms, and N_{K} is the number of trapped potassium atoms.[33] By fitting the curve of MOT loading as shown in Fig. 5(a), we get the β' value of dark MOT smaller than bright MOT, which reveals the advantage of dual dark MOT by reducing the light-assisted collision losses between trapped potassium and rubidium.[34]

Consider that the efficiency of evaporative cooling process of the ^{40}K cloud in two-species ^{87}Rb and ^{40}K mainly depends on the different loading time of ^{87}Rb and ^{40}K. We also perform the optimization of the different loading time of ^{87}Rb and ^{40}K via dark MOT loading. The ^{40}K number of atoms and density as the function of the loading time of ^{40}K and ^{87}Rb is shown in Figs. 6(a) and 6(b), respectively. We can find that the ^{40}K number of the atoms reach the maximum when the loading time of ^{40}K is larger than 60 s and the loading time of ^{87}Rb is between 1 s and 2 s.

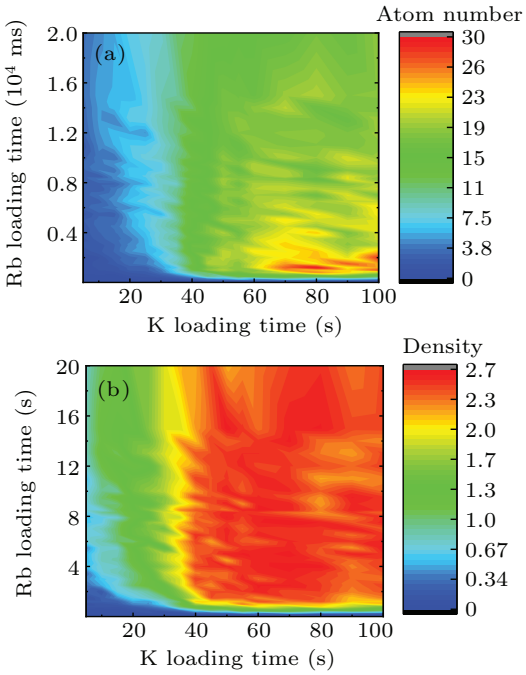

Fig. 6. The optimization of rubidium and potassium loading time. (a) ^{40}K atom numbers and (b) optical density as the function of rubidium and potassium loading time by dark MOT loading. Horizontal axis represents for the Rb loading time, vertical axis represents for the ^{40}K loading time, and color gradient represents the number and density of ^{40}K atoms, respectively.

After evaporative cooling in the hybrid magnetic trap, the atoms with high numbers and high density are then transferred in a 1064 nm far-off-resonant optical dipole trap for further evaporation.[35] Quantum degenerate of ^{87}Rb and ^{40}K atoms can be realized via evaporation in optical dipole trap. We realize around $N = 1.2 \times 10^6$ ultracold ^{87}Rb atoms and around $N = 2.1 \times 10^6$ ultracold ^{40}K atoms at a temperature of $0.36T_{\mathrm{F}}$ in Rb–K mixture simultaneously, where the Fermi temperature is defined by $T_{\mathrm{F}} = \hbar\bar{\omega}(6N)^{1/3}/k_{\mathrm{B}}$. Here $\bar{\omega} = (\omega_x\omega_y\omega_z)^{1/3} \simeq 2\pi \times 80$ Hz is the geometric mean of the optical trap in our experiment, N is the particle number of ^{40}K atoms, and k_{B} is the Boltzmann's constant.

In conclusion, we have constructed the dual dark MOT of ^{87}Rb and ^{40}K, which makes ^{87}Rb and ^{40}K atoms gather in the dark state $F = 1$ and $F = 7/2$ in the process of dark MOT loading. The dark MOT of ^{87}Rb is the same as bright MOT for the single specie gas. However, it has a great improvement for the trapping of ^{40}K atoms in two species mixture of ^{87}Rb and ^{40}K. We have also performed the optimization of mixture ratio by control the loading time of Rb and K. The dark MOT is important for us to obtain large number of high-density ^{40}K atoms, which is essential for the further cooling and the realization of quantum gas.

Acknowledgements

Project supported by the National Natural Science Foundation of China (Grant Nos. 12034011, 92065108, 11974224, 12022406, and 12004229), the National Key Research and Development Program of China (Grant No. 2018YFA0307601), the Fund for Shanxi 1331 Project Key Subjects Construction, and the Program of Youth Sanjin Scholar.

References

[1] Ludlow A D, Boyd M M, Ye J, Peik E and Schmidt P O 2015 *Rev. Mod. Phys.* **87** 637
[2] Cronin A D, Schmiedmayer J and Pritchard D E 2009 *Rev. Mod. Phys.* **81** 1051
[3] Nath D, Easwaran R K, Rajalakshmi G and Unnikrishnan C S 2013 *Phys. Rev. A* **88** 053407
[4] Lvovsky A I, Sanders B C and Tittel W 2009 *Nat. Photon.* **3** 706
[5] Hu J Z, Urvoy A, Vendeiro Z, Crépel V, Chen W L and Vuletić V 2017 *Science* **358** 1078
[6] Bloch I, Dalibard J and Zwerger W 2008 *Rev. Mod. Phys.* **80** 885
[7] Bloch I, Dalibard J and Sylvain 2012 *Nat. Phys.* **8** 267
[8] Raab E L, Prentiss M, Cable A, Chu S and Pritchard D E 1987 *Phys. Rev. Lett.* **59** 2631
[9] Davis K B, Mewes M, Joffe M A, Andrews M R and Ketterle W 1995 *Phys. Rev. Lett.* **74** 5202
[10] Hess Harald F 1986 *Phys. Rev. B* **34** 3476
[11] Davis K, Mewes M O and Ketterle W 1995 *Appl. Phys. B* **60** 155
[12] Xiong D Z, Wang P J and Fu Z K, Chai S J and Zhang J 2010 *Chin. Opt. Lett.* **8** 627
[13] Norcia M A, Cline J R, Bartolotta J P, Holland M J and Thompson J K 2018 *New J. Phys.* **20** 023021
[14] Bruce G D, Haller E, Peaudecerf B, Cotta D A, Andia M, Wu S, Johnson M Y, Lovett B W and Kuhr S 2017 *J. Phys. B* **50** 095002
[15] Lee H J, Adams C S, Kasevich M and Chu S 1996 *Phys. Rev. Lett.* **76** 2658
[16] Kerman A J, Vuletić V, Chin C and Chu S 1986 *Phys. Rev. B* **34** 3476
[17] Urvoy A, Vendeiro Z, Ramette J, Adiyatullin A and Vuletić V 2019 *Phys. Rev. Lett.* **122** 203202
[18] Solano P, Duan Y H, Chen Y T, Rudelis A, Chin C and Vladan V 2019 *Phys. Rev. Lett.* **123** 173401
[19] Anderson M H, Petrich W, Ensher J R and Cornell E A 1994 *Phys. Rev. A* **50** R3597
[20] Coslovsky J, Afek G, Mil A, Almog I and Davidson N 2017 *Phys. Rev. A* **96** 032713
[21] Ketterle W, Davis K B, Joffe M A, Martin A and Pritchard D E 1993 *Phys. Rev. Lett.* **70** 2253
[22] Wei D, Xiong D Z, Chen H X and Zhang J 2007 *Acta Sinica Quant. Opt.* **46** 56
[23] McCarron D J, King S A and Cornish S L 2008 *Meas Sci. Technol.* **19** 105601
[24] Zhang J, Wei D, Xie C D and Peng K C 2003 *Opt. Express* **11** 1338
[25] Lang R 1982 *IEEE J Quant. Electron.* **18** 976
[26] Angelis M D, Cacciapuoti L, Pierattini G and Tino G M 2003 *Opt. Lasers Eng.* **39** 283
[27] Mishra S R, Tiwari S, Ram S and Mehendale S 2007 *Opt. Eng.* **46** 084002
[28] Pierre-André B and Marc R 1978 *Appl. Opt.* **17** 1080
[29] Cai Y J, Lu X H and Lin Q 2003 *Opt. Lett.* **28** 1084
[30] Devlin J A and Tarbutt M R 2016 *New J. Phys.* **18** 123017
[31] Bloch I, Greiner M, Mandel O, Hänsch T W and Esslinger T 2001 *Phys. Rev. A* **64** 021402
[32] Ferlaino F, D'Errico C, Roati G, Zaccanti M, Inguscio M, Modugno G and Simoni A 2006 *Phys. Rev. A* **73** 040702
[33] Mancini M W, Caires A R, Telles G D, Bagnato V S and Marcassa L G 2004 *Eur. Phys. J. D* **30** 105
[34] Marcassa L G, Telles G D, Muniz S R and Bagnato V S 2000 *Phys. Rev. A* **63** 013413
[35] Chai S J, Wang P J, Fu Z K, Huang L H and Zhang J 2012 *Acta Sinica Quant. Opt.* **18** 171